International Journal of Obesity (2016) **40,** 973–981

www.nature.com/ijo

ORIGINAL ARTICLE

Endoplasmic reticulum-associated degradation of the mouse PC1/3-N222D hypomorph and human PCSK1 mutations contributes to obesity

P Stijnen[1], B Brouwers[1], E Dirkx[1], B Ramos-Molina[1], L Van Lommel[2], F Schuit[2], L Thorrez[3], J Declercq[1] and JWM Creemers[1]

BACKGROUND: The proprotein convertase 1/3 (PC1/3), encoded by *proprotein convertase subtilisin/kexin type 1 (PCSK1)*, cleaves and hence activates several orexigenic and anorexigenic proproteins. Congenital inactivation of *PCSK1* leads to obesity in human but not in mice. However, a mouse model harboring the hypomorphic mutation N222D is obese. It is not clear why the mouse models differ in phenotype.

METHODS: Gene expression analysis was performed with pancreatic islets from *Pcsk1*$^{N222D/N222D}$ mice. Subsequently, biosynthesis, maturation, degradation and activity were studied in islets, pituitary, hypothalamus and cell lines. Coimmunoprecipitation of PC1/3-N222D and human PC1/3 variants associated with obesity with the endoplasmic reticulum (ER) chaperone BiP was studied in cell lines.

RESULTS: Gene expression analysis of islets of *Pcsk1*$^{N222D/N222D}$ mice showed enrichment of gene sets related to the proteasome and the unfolded protein response. Steady-state levels of PC1/3-N222D and in particular the carboxy-terminally processed form were strongly reduced in islets, pituitary and hypothalamus. However, impairment of substrate cleavage was tissue dependent. Proinsulin processing was drastically reduced, while processing of proopiomelanocortin (POMC) to adrenocorticotropic hormone (ACTH) in pituitary was only mildly impaired. Growth hormone expression and IGF-1 levels were normal, indicating near-normal processing of hypothalamic proGHRH. PC1/3-N222D binds to BiP and is rapidly degraded by the proteasome. Analysis of human PC1/3 obesity-associated mutations showed increased binding to BiP and prolonged intracellular retention for all investigated mutations, in particular for PC1/3-T175M, PC1/3-G226R and PC1/3-G593R.

CONCLUSIONS: This study demonstrates that the hypomorphic mutation in *Pcsk1*^{N222D} mice has an effect on catalytic activity in pancreatic islets, pituitary and hypothalamus. Reduced substrate processing activity in *Pcsk1*$^{N222D/N222D}$ mice is due to enhanced degradation in addition to reduced catalytic activity of the mutant. PC1/3-N222D binds to BiP, suggesting impaired folding and reduced stability. Enhanced BiP binding is also observed in several human obesity-associated PC1/3 variants, suggesting a common mechanism.

International Journal of Obesity (2016) **40,** 973–981; doi:10.1038/ijo.2016.3

INTRODUCTION

The *proprotein convertase subtilisin/kexin type 1 (PCSK1)* and the *leptin* genes were the first genes discovered to cause monogenic obesity.[1,2] *PCSK1* encodes the proprotein convertase PC1/3 that belongs to a family of seven serine proteases, which share high resemblance to yeast KEXIN and bacterial subtilisins. All PC members cleave proproteins carboxy-terminal of basic amino-acid motifs.[3,4]

PC1/3 is highly expressed in neural and endocrine tissues such as the hypothalamus, pituitary and the pancreatic islets, where it often colocalizes with PC2 in dense-core granules. PC1/3 activity is necessary for the activation of several prohormones and proneuropeptides. After synthesis and signal peptide removal, the resulting zymogen proPC1/3 (95 kDa) requires autocatalytic cleavage of the prodomain at two sites.[5,6] The first cleavage is necessary for exit out the endoplasmic reticulum (ER). The second cleavage is predicted to occur in the Golgi and leads to the release of the prodomain, rendering the enzyme active against substrates *in trans*. Late in the secretory pathway PC1/3 can undergo carboxy-terminal cleavages at two possible positions, which results in an intermediate (74 kDa) or a smaller, less stable but more active form of PC1/3 (66 kDa).

Many PC1/3 substrates are involved in glucose homeostasis, feeding behavior and energy homeostasis. Rare and common polymorphisms in *PCSK1* have been associated with obesity, increased body mass index, altered glucose homeostasis, proinsulin disorders, fat oxidation and postabsorptive resting energy expenditure.[7–14] Complete lack of PC1/3 causes a severe block in neuroendocrine proprotein processing, leading to a multihormonal disorder. In total, 20 patients with congenital PC1/3 deficiency have been identified.[1,6,14–19] In early childhood, patients become severely obese. It is generally assumed that blocked processing of anorexigenic substrates causes hyperphagia and hence obesity, as demonstrated in *an ad libitum* test meal.[15] Most patients also present with severe malabsorptive diarrhea and consequential metabolic acidosis.[6,14,15] The patients develop a complex endocrinopathy marked by growth hormone deficiency,

[1]Laboratory for Biochemical Neuroendocrinology, Department of Human Genetics, KU Leuven, Leuven, Belgium; [2]Gene Expression Unit, Department of Cellular and Molecular Medicine, KU Leuven, Leuven, Belgium and [3]Department of Development and Regeneration, KU Leuven, Leuven, Belgium. Correspondence: Professor JWM Creemers, Laboratory for Biochemical Neuroendocrinology, Department of Human Genetics, KU Leuven, Campus Gasthuisberg O&N1, Box 602 Herestraat 49, Leuven 3000, Belgium.
E-mail: john.creemers@med.kuleuven.be
Received 29 June 2015; revised 3 December 2015; accepted 22 December 2015; accepted article preview online 20 January 2016; advance online publication, 23 February 2016

hypocortisolemia, hypothyroidism, hypogonadotropic hypogonadism and diabetes insipidus, albeit with large patient to patient variations.

In 2002, the *Pcsk1* knockout mouse model was reported not to be obese but growth retarded due to a block of proGHRH processing in the hypothalamus.[20] The mouse model is marked by a combination of complete and partial block of processing of neuroendocrine substrates. In a forward genetic screen using *N*-ethyl-*N*-nitrosourea as a mutagen, the N222D mutation in mouse PC1/3 was reported to cause obesity in a dominant manner when mice were fed a high fat diet (HFD).[21] *In vitro*, human PC1/3-N222D was reported to cause a 34–50% decrease in activity.[21] This suggested that a reduction in PC1/3 activity of 25% or less in heterozygous N222D mice causes obesity, while loss of 100% activity in PC1/3 does not. A molecular explanation for this apparent paradox has not been found. Recently, eight novel heterozygous mutations in *PCSK1* have been reported to predispose to obesity.[13] It was shown that five of these mutations, as well as the mouse N222D mutation and the polygenic SNP rs6232 coding for N221D, cluster around the Calcium 1 binding site (Ca-1) in PC1/3. This site is known to be important for structural stability of subtilisin, the prokaryote ortholog of PC1/3.[22] In this study, we have investigated the pathogenesis of obesity in the PC1/3-N222D mouse model and whether this molecular mechanism also applies to common and rare human *PCSK1* mutations.

MATERIALS AND METHODS

Animal breeding

The C57BL/6 J-Pcsk1^{N222D}/J mouse model, hereafter referred to as *Pcsk1*$^{N222D/N222D}$, was obtained from Jackson Laboratories (Mount Desert Island, ME, USA). PC1/3-null mice[20] (*CD1-PCSK1*$^{WT/KO}$) were obtained from Dr Robert Day (Sherbrooke, Canada). The mice were housed in the specific pathogen free facility of the KU Leuven and all experiments were conducted with *a priori* approval by the local ethical committee (P072/2011). All experiments were conducted on 14-week-old mice, which had received 4 weeks HFD (45% calories from fat) or normal fat diet (11% calories from fat).

Tissue isolation

Pancreatic islets were isolated for RNA isolation as previously described.[23] For the collection of protein samples, the pancreata were locally injected with Liberase TL (Roche Applied Science, Basel, Switzerland) as previously described.[24] Pituitaries and hypothalami were dissected macroscopically, and all tissues were snap-frozen in liquid nitrogen till later use.

Site-directed mutagenesis

For *in vitro* experiments, the previously described human *PCSK1* constructs were adapted.[13] The hypermorphic mutation in this construct[25] was mutated back to wild type using site-directed mutagenesis. Similarly to the human constructs, a FLAG tag was inserted carboxy-terminal of the prodomain of mouse PC1/3; and the N222D mutation was created using QuickChange site directed mutagenesis kit (Stratagene, La Jolla, CA, USA). Constructs were verified by Sanger sequencing. For viral transduction, the constructs were cloned into the pLenti-GFP-PURO[26] eukaryotic expression vector where the GFP gene was replaced by either human or mouse *PCSK1* constructs.

Cell culture and viral transduction

For virus production, HEK293T cells were triple transfected with 0.1 μg Δ8.9, 0.9 μg VSV-G and pLenti-empty, pLenti-*Pcsk1* or pLenti-*Pcsk1*-N222D (for 10 cm^2) using Xtreme gene 9 transfection reagent. Insulinoma βTC3 cells were transduced with lentivirus and selected using 2 μg ml^{-1} puromycin for 2 days. The activity measurement was conducted as described previously.[12]

Immunoblotting and immunoprecipitation

Recombinant PC1/3 with Flag tag was immunoprecipitated as described previously using the FlagM2 antibody (Sigma-Aldrich, Saint Louis, MO, USA).[13] For intracellular PC1/3, cells were lysed in lysis buffer (150 mM Tris-HCl pH 7.4, 50 mM NaCl, 1% Triton-X-100, 1 × Complete Mini Protease inhibitors (Roche Applied Science, Basel, Switzerland). Immunoprecipitated PC1/3 or other protein samples were separated by SDS-PAGE, and western blot was conducted with antibodies for FlagM2 (Sigma-Aldrich), BiP (CS 3177), IRE1alpha(CS 3294), eIF2alpha (CS 2103) (Cell Signaling, Danvers, MA, USA), PC1/3[ref. 1] and N-term. PC1/3 (kind gift from Dr Iris Lindberg), insulin #3B7 (kind gift from Dr John Hutton, Denver, USA), P-IRE1alpha (NB100-2323), ATF6 (IMG-273) (Novus Biologicals, Littleton, CO, USA), P-eIF2alpha[27] and adrenocorticotropic hormone (ACTH) (A1A12, kind gift from Dr Anne White).

Metabolic labeling

Cells were metabolically labeled with 100 μCi ^{35}S methionine/cysteine (Easytag express protein labeling mixture, specific activity, 1175 Ci mmol^{-1}; Perkin-Elmer, Waltham, MA, USA) for 30 min and chased in RPMI-1640 containing an excess (0.4 mM) of unlabeled methionine and cysteine (both 0.4 mM) for the indicated times. Cells were lysed in 1 ml lysis buffer. PC1/3 was immunoprecipitated as described above and samples were run on SDS-PAGE, followed by autoradiography. For inhibition of the proteasome and the lysosome, the inhibitors were added during starvation, pulse and chase of the cells. MG132 was dissolved in DMSO (1000 ×), and used at a final concentration of 50 μM. Leupeptin and chloroquine (Sigma-Aldrich) were added at a final concentration of 200 μM and 100 μg ml^{-1}, respectively.

RNA extraction and Microarray

Total RNA from islets was isolated using Absolutely RNA microprep kit (Agilent, Santa Clara, CA, USA) according to the manufacturer's protocol. RNA quantity and quality were assessed using a spectrophotometer (ND-1000; NanoDrop Technologies, Wilmington, DE, USA) and a Bioanalyser (2100; Agilent), respectively. Total RNA (100 ng) of isolated islets was used to hybridize Mogene_1.0_ST array (Affymetrix, Santa Clara, CA, USA) according to the manufacturer's protocol manual 4425209RevB as described previously.[23] For RT-qPCR, RNA was isolated using the RNAxs kit (Machery-Nagel, Düren, Germany). cDNA was prepared from 250 or 500 ng RNA using the iScript cDNA synthesis kit (Bio-Rad, Hercules, CA, USA).

Pathway analysis

Linear expression values from the microarrays served as an input in Gene Set Enrichment Analysis 2.013 (GSEA).[28] This tool identifies whether predefined gene sets are statistically significantly different between two biological states. Enrichment analysis was carried out using the curated canonical pathways database present at Broad Institute. Enriched gene sets were clustered using Enrichment Map in Cytoscape 3.20.[29] The similarity coefficient between gene sets was used as a proxy for spring-electric layout using AllegroLayout plugin. For analysis of enriched DNA-binding motifs, the data were loaded in Multi experiment viewer (MeV, TM4).[30] Data were median/center normalized and analyzed with Significance analysis of Microarrays. The 100 genes containing the highest observed *d*-score were selected for iREGULON analysis.[31] Enrichment score threshold was set at 3.0, receiver operator curve threshold for area under the curve at 0.03 and maximum false discovery rate (FDR) on motif similarity at 0.001.

RT-qPCR

Real-time RT-qPCR was performed using iQ SYBR Green Supermix (Bio-Rad). Forty cycles of annealing/extension for 1 min at 60 °C were carried out with the MyiQ single color real-time PCR detection system (Bio-Rad). Specific primers were designed using primer BLAST (NCBI). Primer efficiencies were tested using serial dilution of cDNA. Reference genes were selected from the microarray data, and stability was assessed with Normfinder.[32] Primer sequences and efficiencies are listed in Supplementary Table 1. Gene expression was calculated as described by Hellemans *et al.*[33]

Metabolic measurements

Insulin growth factor 1 (IGF-1) content was measured using the Quantikine ELISA Mouse/Rat IGF-I Immunoassay (R&D Systems, Minneapolis, MN, USA) according to the manufacturer's protocol. Measurement of total pancreas insulin content was performed as described previously.[24] Total immunoreactive insulin (proinsulin, insulin and processing intermediates) and specific mature insulin content were determined using the Rat High Range Insulin ELISA and the Mouse Ultrasensitive Insulin ELISA (Mercodia, Uppsala, Sweden), respectively. Intraperitoneal glucose and insulin tolerance tests were conducted as described previously.[24]

Immunohistochemistry

Tissues were isolated and fixed in 4% formaldehyde as previously described.[24] Tissue slides of 5 μM thickness were deparaffinized, rehydrated and double-stained for insulin (A0564, Dako, Glostrup, Denmark) and KI67 (15580, Abcam, Cambridge, UK) to assess proliferating cells or for apoptotic cells using the TUNEL assay (In Situ Cell Death Detection Kit (fluorescein, Roche Applied Science) according to the manufacturer's protocols.

Statistics

All data are represented as mean ± s.e.m. unless indicated otherwise. Differences between groups were tested using unpaired two-tailed T tests unless indicated otherwise. Sample size was determined, based upon the type of experiment. Differences in variance were tested with the Levene's test.

RESULTS

Phenotypic analysis of Pcsk1$^{N222D/N222D}$ shows a severe reduction in proinsulin processing

The activity of PC1/3-N222D was assessed using an *in vitro* enzymatic assay (Figure 1a). Human PC1/3-N222D had residual activity of approximately 50%, conform previous reports.[21,34] However, the activity of mouse PC1/3-N222D was reduced to background levels in the conditioned medium. Furthermore, little mouse PC1/3-N222D was secreted. These results indicate that the PC1/3 activity in *Pcsk1*$^{N222D/N222D}$ mice is more severely impaired than assumed in the original publication where recombinant human PC1/3-N222D was used.[21] Therefore, substrate processing was analyzed in the hypothalamus, pituitary and pancreatic islets of *Pcsk1*$^{WT/N222D}$ and *Pcsk1*$^{N222D/N222D}$ mice. *Pcsk1*$^{N222D/N222D}$ mice appeared normal in size, had normal plasma IGF-1 concentrations and normal pituitary *Gh* expression (Figures 1b and c). However, hypothalamic *Ghrh* expression was significantly increased (~40%) in *Pcsk1*$^{N222D/N222D}$ mice (Figure 1b). These results differ from those obtained with the *Pcsk1* knockout mice, which have decreased GH and IGF-1 levels and doubled proGHRH protein as a consequence of blocked proGHRH processing.[20] In the pituitary, proopiomelanocortin (POMC) was fully processed to 4.5–13 kDa ACTH; however, the ratio of the intermediate cleavage product 21–23 kDa proACTH and POMC was significantly increased in pituitaries of *Pcsk1*$^{N222D/N222D}$ mice (Figure 1d). Total pancreatic immunoreactive insulin (including proinsulin and cleavage intermediates) after normal diet was more than doubled (2.81-fold, $P < 0.05$) in *Pcsk1*$^{N222D/N222D}$ mice compared with wild-type littermates while specific insulin content was comparable across genotypes (Figure 1e). Western blot analysis on islets confirmed that proinsulin was highly increased in the islets from *Pcsk1*$^{N222D/N222D}$ (Figure 1f). Using non-reducing conditions, a decrease in insulin and an increase in insulin precursors are observed (Figure 1g). Metabolic labeling showed that proinsulin was not processed to detectable insulin levels in pancreatic islets from *Pcsk1*$^{N222D/N222D}$ mice after a 1-h chase (Figure 1h). Glucose tolerance tests in *Pcsk1*$^{N222D/N222D}$ mice were normal after a control diet, but impaired after 4 weeks on an HFD (Supplementary Figure 1A), indicating that proinsulin processing is severely perturbed when the metabolic load increases. Similarly, body weight was comparable in adult mice on normal fat diet, but significantly increased after HFD in *Pcsk1*$^{N222D/N222D}$ in comparison with wild-type littermates (Supplementary Figure 1B) Taken together, these results show that despite severely reduced activity of PC1/3-N222D *in vitro*, no evidence was found for physiologically relevant reductions in substrate processing in the GHRH/GH/IGF-1 axis and POMC to ACTH processing, despite increased precursor expression. Processing of proinsulin in pancreatic islets was more severely reduced, but only affected glucose homeostasis after HFD challenge.

Gene expression analysis shows upregulation of unfolded protein response and proteasomal gene sets

The gene expression profile of pancreatic islets from mice fed an HFD was determined to investigate the impact of PC1/3-N222D (Figure 2a). Nine clusters of gene sets were identified that were significantly enriched in the pancreatic islets of the *Pcsk1*$^{N222D/N222D}$ mice (FDR-q < 0.01 and $P < 0.005$), using GSEA. The largest cluster consisted of gene sets linked to proteasomal protein degradation. One cluster contained gene sets for unfolded protein response (UPR) and XBP1s activation. Gene expression data were used to identify activated transcriptional pathways. The enrichment of DNA-binding motifs in the 100 most differentially regulated genes (Supplementary Table 2) from the microarray was analyzed using iREGULON.[31] The top 10 enriched DNA-binding motifs are targets of ATF6, XBP1, CREB3, CREB3L1 or CREB3L2 and activate transcription of up to 21 genes from the input list (Table 1). CREB3 (OASIS), CREB3L1 (LUMAN) and CREB3L2 are bZIP transcription factors belonging to the OASIS family and share high homology with ATF6.[35] The observed enrichment of proteasomal and UPR gene sets indicates that PC1/3-N222D might be degraded through ER-associated degradation (ERAD). This was investigated by western blot analysis of PC1/3 in the hypothalamus, pituitary and pancreatic islets (Figure 2). In all these tissues, a decrease in 66 kDa PC1/3-N222D could be observed, while the much less abundant 87 kDa form was less affected.

PC1/3-N222D is rapidly degraded by the proteasome

The decreased immunoreactivity of 66 kDa PC1/3 in *Pcsk1*$^{N222D/N222D}$ tissues was further investigated in transiently transfected HEK293T and stably transduced insulinoma βTC3 cells (Figures 3a–d). In βTC3 cells, PC1/3-N222D did partly mature, but no carboxy-terminally processed form was present and a clear decrease was observed after 8 h of chase (Figure 3a). To investigate whether PC1/3-N222D is degraded by proteasomes or lysosomes, pulse chase experiments in the presence of either the proteasomal inhibitor MG132 or the lysosomal inhibitors chloroquine and leupeptin (C/L) were performed (Figure 3b). Degradation of PC1/3-N222D in βTC3 cells was mostly prevented by proteasomal inhibition with little effect of the lysosomal inhibitors (Figure 3b). In HEK293T cells, mainly proPC1/3-N222D was detected while wild-type PC1/3 rapidly matured (Figure 3c). In addition, little intracellular immunoreactive PC1/3-N222D remained after 4 h of chase, while considerable amounts of wild-type PC1/3 were still detectable even after 8 h. Taken together, the low amounts of PC1/3-N222D in the mouse model are most likely due to increased proteasomal degradation, as observed for recombinant PC1/3-N222D in cell lines. The glycosylation of mouse PC1/3-N222D was analyzed to identify whether PC1/3-N222D is able to exit the ER (Supplementary Figure 3). This shows that PC1/3 is not complex glycosylated in HEK293T cells and that glycan is endoglycosidase H sensitive, indicating that most of PC1/3-N222D resides in the ER.

If PC1/3-N222D cannot fold stably, then it is likely bound to the ER chaperone protein BiP, which binds transiently to unfolded proteins and more stably to misfolded proteins.[36] To test this hypothesis, PC1/3 was immunoprecipitated from cell lysates of stably transduced βTC3 cells, and co-immunoprecipitated BiP was

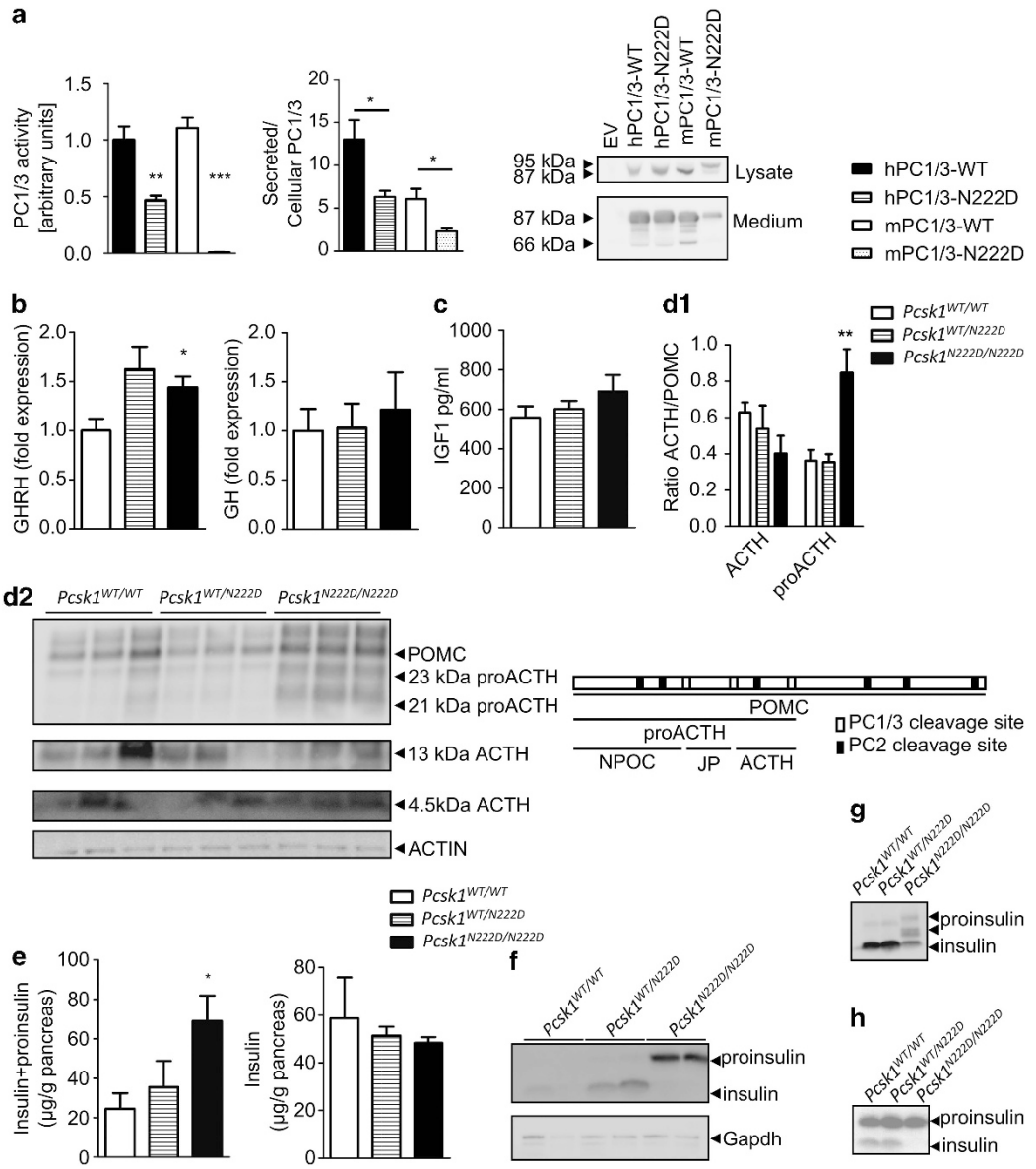

Figure 1. Mouse PC1/3-N222D does not show activity *in vitro*, but does not physiologically impair substrate processing. Human and mouse PC1/3 constructs with or without the N222D mutation were transfected in HEK293T cells. (**a**) Conditioned medium and cell lysates were used for western blot, and density of the bands was measured. The enzymatic activity was measured using a fluorogenic substrate. The PC1/3 activity, relative to protein levels, was normalized to human PC1/3-WT. The amount of PC1/3 in the medium and lysate were measured by densitometry of the western blots. The ratio of secreted/cellular PC1/3 is also depicted. (**a**) Representative western blot for the expression of PC1/3 in HEK293T cells and conditioned medium is shown, $n = 5$. (**b, c**) Assessment of the GHRH-GH-IGF1 axis. (**b**) Relative expression of *Ghrh* and *Gh* measured by RT-qPCR from RNA of mouse hypothalamic or pituitary, respectively, $n = 3–5$. (**c**) Plasma IGF-1 levels as measured by a specific ELISA, $n = 5–8$. (**d1**) Quantification of band densities of different ACTH species (**d2**). Non-glycosylated (4.5 kDa) and glycosylated (13 kDa[50]) ACTH band densities were summed and divided by POMC band densities. Similarly, 21 and 23 kDa bands were counted together as a measure for proACTH. The ratio of proACTH or ACTH over POMC is depicted. (**d2**) Right, a schematic representation of PC1/3 and PC2 cleavage sites in POMC and the specific PC1/3 products, which are formed in pituitary corticotrophs. Left, western blots for ACTH and ACTH precursors from pituitary samples, n=5. Different panels originated from the same blot but were exposed for increasing time intervals with decreasing Mw. (**e**) Proinsulin concentration is increased in islets of Langerhans ($n = 5–6$). Left, total insulin levels measured by an ELISA kit which cross-reacts with proinsulin. The total amount of pancreatic insulin and proinsulin species is increased by 2.8-fold. Right, specific insulin levels measured by ELISA. (**f**) Reducing western blot for insulin in islets of Langerhans shows increased proinsulin species in Pcsk1$^{N222D/N222D}$ islets. (**g**) Non-reducing western blot of islets of Langerhans shows increased insulin precursors in Pcsk1$^{N222D/N222D}$ islets. (**h**) Proinsulin processing in pancreatic islets after 30 min of radiolabeling and 1 h of chase. $^*P < 0.05$; $^{**}P < 0.01$; $^{***}P < 0.001$; data are represented as mean ± s.e.m.

detected by western blot (Figure 3d). Considerable amounts of BiP co-immunoprecipitated with PC1/3-N222D, similar to the previously reported null mutant PC1/3-G593R, which has previously been shown to be retained in the ER.[1] Less, but clearly detectable amounts of BiP co-immunoprecipitated with wild-type PC1/3. These data suggest that PC1/3 requires BiP for folding and that PC1/3-N222D is indeed prone to misfolding and hence has a prolonged interaction with BiP.

To determine whether PC1/3-N222D misfolding causes ER stress, the activation of the three canonical ER stress sensors: ATF6α, IRE1α and elf2α as a marker for PERK, was assessed. No difference in phosphorylation of the latter two was observed

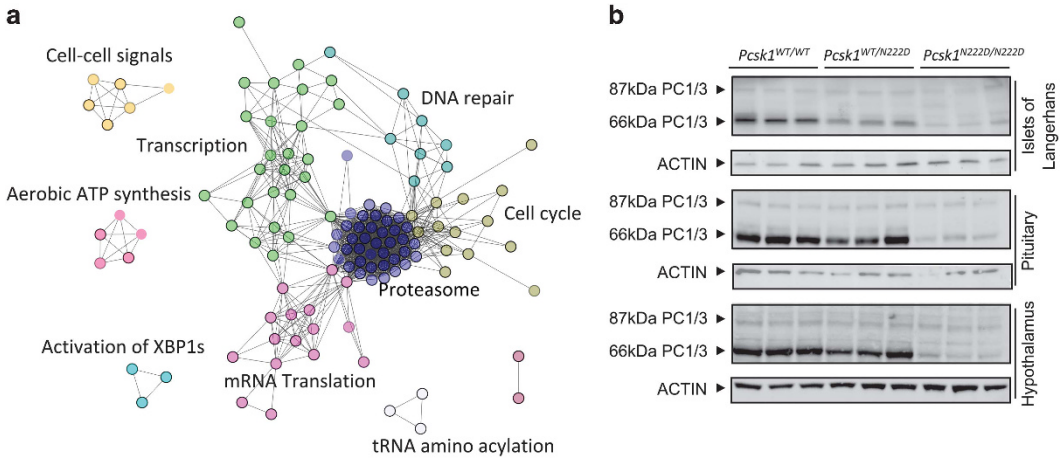

Figure 2. Decreased 66 kDa PC1/3 protein coincides with enrichment of proteasomal gene sets in gene expression analysis**.** (**a**) RNA from pancreatic islets from female mice fed an HFD for 4 weeks was used for microarray expression analysis. Linear expression values served as an input in GSEA 2.013.[28] Enriched gene sets were clustered using Enrichment Map in Cytoscape 3.20.[29] Each node represents one gene set, the color of the node border represents FDR-q value with white color equals FDR-q = 0.05 and black equals FDR-q = 0. Overlap coefficient cutoff was set at 0.5, *P*-value cutoff was set at 0.005 and FDR-q cutoff was set at 0.05. For each cluster, leading edge analysis was performed and most relevant gene set was used to name the clusters. (**b**) Western blot for PC1/3 in pituitary, hypothalamic and pancreatic islets from female mice fed an HFD for 4 weeks. Arrowheads indicate specific bands. Similar results were observed for tissues of mice fed a normal fat diet.

Table 1. Enrichment of DNA-binding motifs in increased expressed genes

# Rank	*Motif id*	*AUC*[a]	*NES*	*Transcription factor*
1	taipale-NNNGMCACGTCATC-XBP1-DBD	0.11	10.18	Xbp1,Creb3,Creb3l1,Atf6,Atf6b,Creb3l2
2	taipale-NTGCCACGTCAYCN-CREB3-full	0.11	9.91	Creb3,Xbp1,Creb3l1,Atf6,Atf6b,Creb3l2
3	taipale-NTGCCACGTCANCA-CREB3L1-DBD	0.10	9.25	Creb3l1,Xbp1,Creb3,Atf6,Atf6b,Creb3l2
4	taipale-TGCCACGTCATCA-Creb3l2-DBD	0.10	9.18	Taf9,Creb3l1,Creb3,Atf6,Atf6b,Creb3l2
5	taipale-NTGCCACGTCANCA-CREB3L1-full	0.09	8.46	Creb3l1,Xbp1,Creb3,Atf6,Atf6b,Creb3l2
6	transfac_public-M00356	0.09	7.95	Xbp1,Creb3,Creb3l1,Atf6,Atf6b,Creb3l2
7	transfac_pro-M00936	0.08	6.98	E4f1
8	transfac_pro-M01815	0.08	6.51	
9	transfac_public-M00483	0.07	6.30	Atf6,Creb3,Atf6b,Creb3l1
10	CrebA_SANGER_5_FBgn0004396	0.07	6.24	Creb3l1,Creb3l2,Creb3,Atf6,Atf6b,Arnt2

Abbreviation: NES, normalized enrichment score. [a]AUC: area under the curve is used for motif detection for which the input genes are enriched at the top of the ranking.

(Supplementary Figure 2). However, cleaved ATF6α was increased in the pancreatic islets of heterozygous mice, but not in homozygous mice. No differences were observed in the pituitaries and hypothalami (Figures 3e and f).

UPR activation was further investigated using RT-qPCR for downstream factors of XBP1 and ATF6α in the pancreatic islets (Figure 3g). No significant upregulation could be observed for *Xbp1s*, but a downstream target *Erdj4* showed a significantly increased expression in both heterozygous and homozygous islets. *Erdj4* encodes a co-chaperone for BiP, which is correlated with ERAD.[37] *G2e3* and *Serp1* were only upregulated in heterozygous mice. *G2e3* is an E3 ubiqituin ligase and *Serp1* encodes for an ER membrane protein involved in UPR. This observation was not due to loss of PC1/3 activity in the pancreatic islets, as no differences were observed for pancreatic islets of CD1-*Pcsk1*$^{WT/KO}$ mice.

PC1/3-N222D expression causes reduced proliferation of pancreatic β cells

Cell cycle and cell cycle-related processes were found to be different in the GSEA. This suggests that PC1/3-N222D misfolding could have an effect on β-cell proliferation and viability. Immunohistochemistry for the cell proliferation marker KI67 showed a severe decrease in β-cell proliferation in *Pcsk1*$^{WT/N222D}$ and *Pcsk1*$^{N22D/N222D}$ mice when fed an HFD for 4 weeks (Figures 4a and c). TUNEL staining showed no difference in the amount of apoptotic β cells (Figures 4b and c). This suggests that on HFD β cells expressing PC1/3-N222D are not able to compensate for the increased demand of insulin by increasing β-cell proliferation.

ER retention of human PC1/3 mutants correlates with a higher binding to BiP

The effect of human obesity-associated mutations in PC1/3 on folding was investigated by co-immunoprecipitation of BiP. The eight previously reported heterozygous mutations,[13] together with the common polymorphisms PC1/3-N221D, PC1/3-N221D-Q665E-S690T and the null mutant PC1/3-G593R, were transiently expressed in HEK293T cells. PC1/3-T175M and PC1/3-G593R bound significantly increased amounts of BiP, while several other mutants showed moderately increased binding to BiP, albeit not significantly more than wild-type PC1/3 (Figures 5a and b). Second, the effect of PC1/3 mutation on cell retention was investigated (Figure 5c). After 1-h chase, most wild-type PC1/3 was secreted from the cells, while all PC1/3 mutants were still detectable in the cell. Taken together, the majority of human

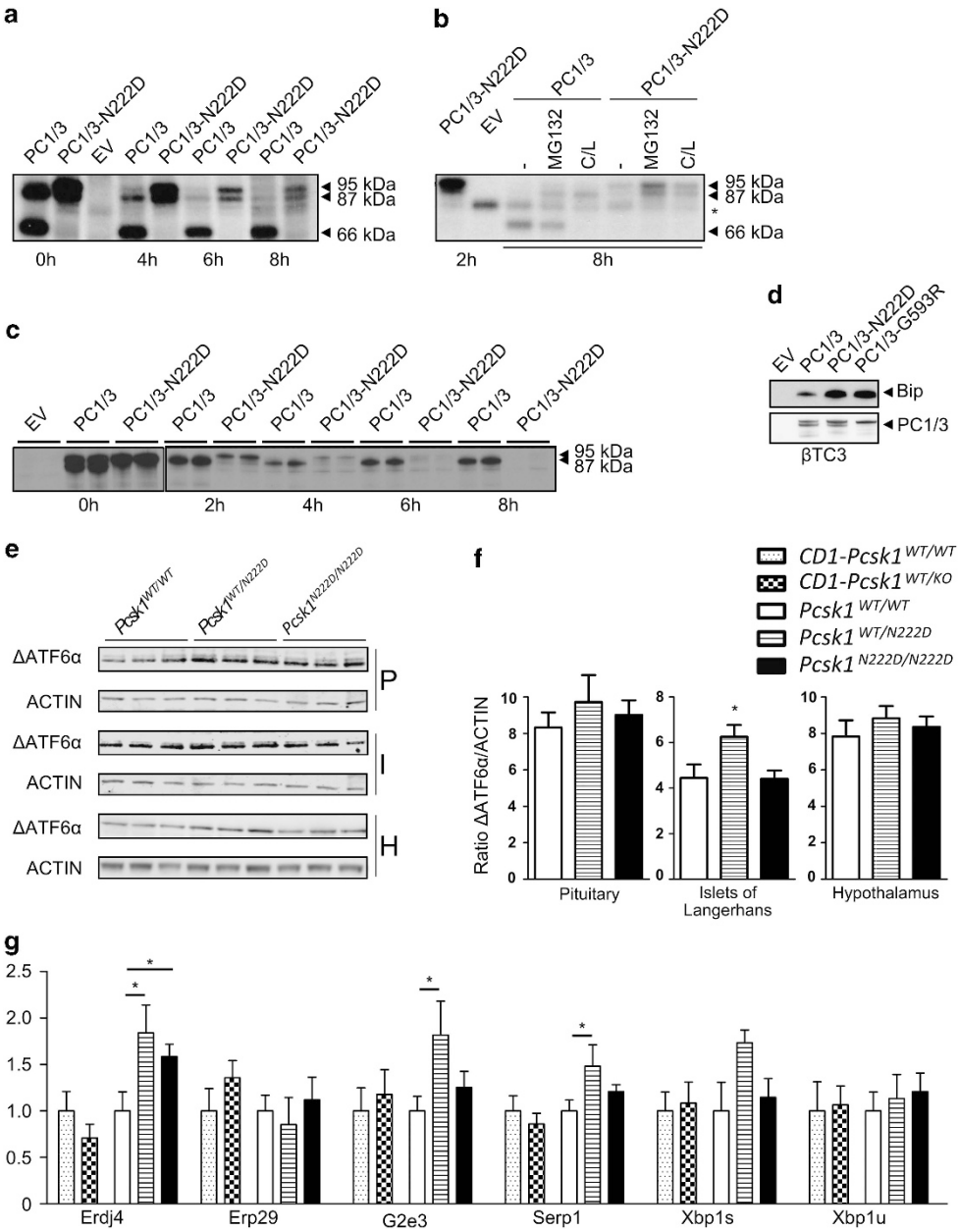

Figure 3. PC1/3-N222D binds BiP, is degraded by the proteasome and leads to increased ΔATF6α levels. Immunoprecipitation of mouse PC1/3 and PC1/3-N222D from βTC3 (**a, b**) cells or HEK293T (**c**) cells. Cells were metabolically labeled for 30 min and chased for the indicated times. (**b**) Cells were treated with proteasomal (MG132) and lysosomal inhibitors (chloroquine and leupeptin [C/L]) as indicated. (**d**) PC1/3, PC1/3-N222D and human PC1/3-G593R were immunoprecipitated from βTC3 cells, and co-immunoprecipitated BiP was detected by western blot. * indicates an aspecific band. EV, empty vector. (**e**) Western blot was performed with lysates from pancreatic islets, pituitary and hypothalamus tissues from mice fed an HFD for 4 weeks. (**f**) Ratio of ΔATF6α/ACTIN calculated from western blots, $n=6$ for islets, $n=8$ for pituitary and hypothalamus. A representative western blot is shown in (**e**). (**g**) RT-qPCR analysis of target genes of Xbp1-spliced (Xbp1s) on cDNA from pancreatic islets of HFD-fed mice. $N=7$–9. Data are depicted as mean ± s.e.m., * indicates $P<0.05$. Data from RT-qPCR were statistically tested with a one-sided *T*-test.

variants showed either increased binding to BiP or delayed secretion or both.

DISCUSSION

In this study, we have investigated the effect of the N222D mutation on PC1/3 biology and substrate processing in a mouse model for HFD-induced obesity. We have shown that PC1/3-N222D is prone to misfolding, binds to the ER chaperone BiP and is degraded by the proteasome. The amount of 66 kDa carboxy-terminally processed PC1/3-N222D was decreased in the pancreatic islets, pituitary and hypothalamus. Processing was most severely affected in the pancreatic islets resulting in reduced amounts of insulin and a large amount of proinsulin. Processing of proGHRH in the hypothalamus and POMC to ACTH in the pituitary was not sufficiently affected to have physiological consequences. Several rare obesity-associated human PC1/3 mutants also showed increased BiP binding and prolonged ER retention, suggesting a common mechanism.

Amino acid N222 in PC1/3 is predicted to be one of the side chain ligands of the calcium in the Ca-1 binding site.[13] This site is conserved in both PCs and bacterial subtilisins, and has been

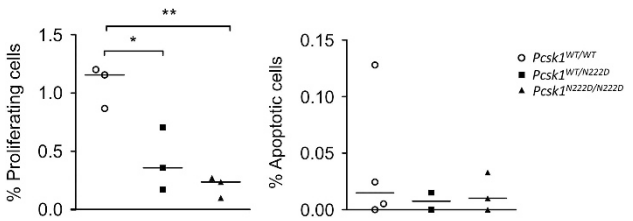

Figure 4. Decreased proliferation of pancreatic β cells in *Pcsk1*$^{N222D/N222D}$ mice. Paraffin-embedded pancreata were used for double immunofluorescence staining. The amount of cells expressing insulin and/or the proliferation marker KI67 was counted, and the ratio of proliferating cells calculated. Approximately 3000 β cells were counted per mouse. Similarly, pancreatic tissue was used to count the amount of apoptotic β cells in the pancreatic islets. Approximately 10 000 cells were counted in a minimum of 50 islets per mouse. Each dot represents the percent proliferating/apoptotic β cells per mouse. Data are presented as median and individual data points. Statistical analyses were conducted with Mann–Whitney *U* test. $*P < 0.05$, $**P < 0.01$.

shown to be important for stability.[22] The prolonged interaction with BiP and the rapid targeting for ERAD of PC1/3-N222D are consistent with impaired stability. It is striking that of the eight recently described obesity-associated mutants, five are located near (M125I, T175M, N180S and Y181H) or directly ligated to (G226R) the Ca-1.[13] Furthermore, one of the common polymorphisms linked to obesity (N221D)[34] is located adjacent to N222D and is therefore likely to have an effect on the stability of Ca-1 binding site as well. However, other mutations (T558A and S325N) not located near the Ca-1 binding site also showed increased intracellular retention, indicating that the Ca-1 binding site is not solely responsible for protein stability.

Why mouse PC1/3 is more severely affected by the N222D mutation than human PC1/3 is unclear, but may be related to N-glycosylation. Mouse PC1/3 contains two functional N-glycan chains and human PC1/3 only one.[13,38] Thermodynamic analysis has shown that N-glycosylation of proteins affects protein folding by destabilization of the unfolded state and correlates with the number of glycans.[39] As a consequence, the two N-glycans in mouse PC1/3 might make the protein more sensitive to misfolding as a consequence of the N222D mutation. Recently, Prabhu *et al*.[40] showed that mouse PC1/3-N222D is degraded by the proteasome and is retained to the ER, which agrees with our observations. However, Prabhu *et al*. also reported that the PC1/3-N222D has an extended intracellular half-life in N2A cells, in contrast to our data in HEK293T and βTC3 cells. We found that PC1/3-N222D has a shorter half-life consistent with the observation that PC1/3-N222D is degraded. This discrepancy can most likely be explained by the fact that Prabhu *et al*. used a construct where the carboxy-terminal cleavage site was mutated.

Carboxy-terminal processing of PC1/3 results in a more active, but also less stable enzyme,[41] and it is therefore not surprising that this 66 kDa form is virtually absent in *Pcsk1*$^{N222D/N222D}$ mice. As a consequence, proinsulin processing was severely delayed, including mildly decreased mature insulin levels. Glucose tolerance was normal when mice were fed a normal diet. Residual insulin activity from mature insulin and proinsulin is sufficient to maintain homeostasis. However, when fed an HFD mice became obese, glucose intolerant and had a decreased islet β-cell proliferation. Probably, the reduced enzymatic activity and the presence of PC1/3-N222D in the tissues result in an insufficient proinsulin processing leading to islet decompensation. Additionally, insulin-producing β cells of *Pcsk1*$^{N222D/N222D}$ mice may be more sensitive to ER stress.[27] Previously, Lloyd *et al*.[21] showed that the islets of *Pcsk1*$^{N222D/N222D}$ mice were hypertrophic, which was also noted by us during islet isolations. This suggests that during development islets become hypertrophic to cope with the absence of sufficient active insulin. Once the mice are given HFD, the β-cells decompensate and fail to proliferate in response to the increased metabolic demands.

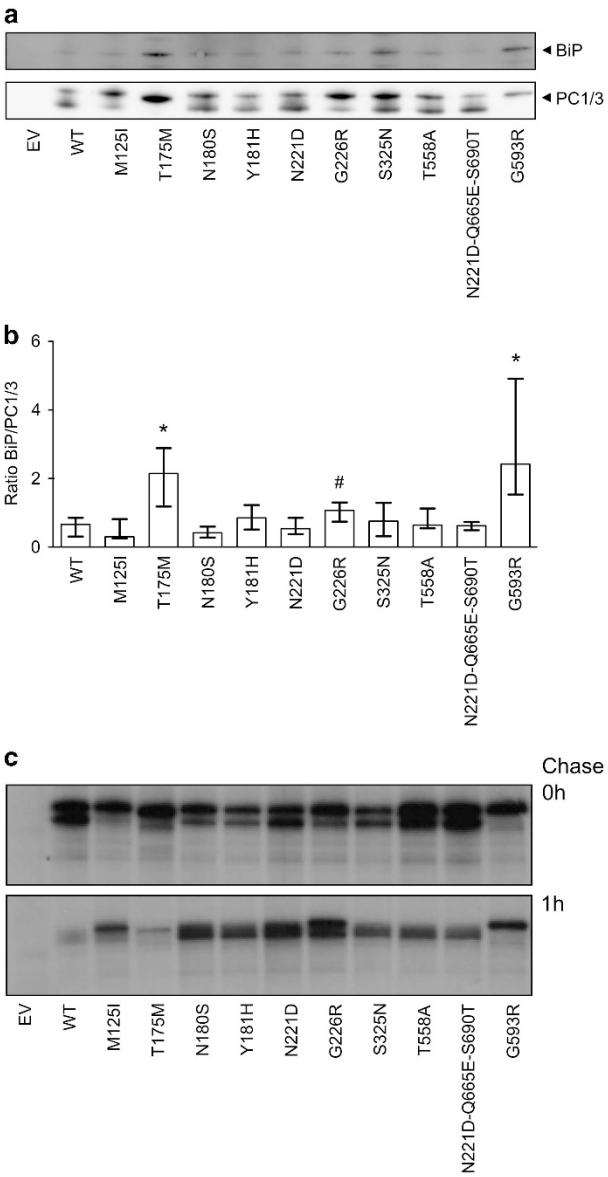

Figure 5. Human PC1/3 mutants bind BiP and are retained in the ER. Human PC1/3 variants were expressed in HEK293T cells, and PC1/3 was immunoprecipitated from the cell lysates. Proteins were separated by SDS-PAGE, and western blot analysis for BiP and PC1/3 was performed. (**a**) Representative image of an immunoprecipitation experiment. (**b**) Ratio of BiP/PC1/3, $n = 7$, median and interquartile range are depicted. Statistical analysis was conducted with Mann–Whitney *U* test. $^{\#}P = 0.06$; $*P < 0.05$. (**c**) HEK293T cells overexpressing PC1/3 mutants were pulsed for 30 min and chased for indicated time points. PC1/3 was immunoprecipitated and separated by SDS-PAGE. A representative experiment is shown, $n = 4$.

The upregulation of ATF6α and increased expression of *Erdj4, G2e3 and Serp1* in *Pcsk1*$^{WT/N222D}$ pancreatic islets indicates a toxic effect of PC1/3-N222D when co-expressed with PC1/3-WT, which could lead to low-grade ER stress in pancreatic islets of *Pcsk1*$^{WT/N222D}$animals. Prabhu *et al*.[40] has shown that co-expression of PC1/3-N222D and PC1/3-WT leads to a small decrease in secretion of PC1/3-WT. It is known for some proteins that oligomerization is a prerequisite for ER exit[42] and that PC1/3 is present in oligomers in

the post ER compartments.[43,44] It is therefore tempting to speculate that PC1/3-N222D/PC1/3-WT heterodimers that are formed in the ER cannot be degraded as efficiently as PC1/3-N222D homodimers, perturb ER exit of PC1/3-WT and hence bind BiP for a prolonged period of time causing a more pronounced UPR. Such a model would also explain the dominant obesity phenotype in *Pcsk1*$^{WT/N222D}$ animals when fed an HFD. Two other proprotein convertases, PC4 and PC7, have also been reported to bind BiP under normal conditions, indicating the need of BiP to assist in folding and prevent aggregation.[45,46] In addition, it has been reported that the expression and function of proprotein convertases and carboxypeptidases are highly dependent on ER homeostasis.[47–49]

Our *in vivo* data support the fact that PC1/3-N222D is still partly functional in the hypothalamus since the GHRH-GH-IGF-1 axis appeared not to be disturbed. This is in clear contrast to the PC1/3-null mice, which displayed a dwarf phenotype as a consequence of unprocessed proGHRH.[20] However, it has been reported that αMSH is nearly twofold decreased in hypothalami of *Pcsk1*$^{N222D/N222D}$ mice, coinciding with hyperphagia.[21] This could mean that the decrease in PC1/3 activity is cell and/or substrate dependent. In addition, the activity of 66 kDa PC1/3 might be required for proinsulin cleavage, whereas 87 kDa PC1/3 activity might be sufficient for other substrates explaining differential cleavage of PC1/3 substrates in the *Pcsk1*$^{N222D/N222D}$ mice. In the pituitary, we found an increased amount of ACTH precursors and normal ACTH levels. In PC1/3-null patients, normal ACTH and decreased cortisol levels were found in plasma as well, accompanied with increased POMC precursors.[6,15] The expression of PC1/3-N222D in the pancreatic islets led to decreased insulin and accumulation of proinsulin, similar to PC1/3-null mice.[20]

In conclusion, our findings show that obesity in *Pcsk1*$^{N222D/N222D}$ mice is caused by misfolding, binding to BiP and proteasomal degradation of PC1/3-N222D, leading to near-complete loss of activity in the pancreatic islets and to a lesser extent in hypothalamus and pituitary. Molecular analysis of this mutant and the human obesity-associated PC1/3 mutations suggest a common mechanism.

CONFLICT OF INTEREST

The authors declare no conflict of interest.

ACKNOWLEDGEMENTS

PS designed the study, researched data and wrote the manuscript. BB researched data and reviewed the manuscript. ED and LV researched data, BR, FS, LT and JD reviewed the manuscript. JWMC wrote the manuscript and is guarantor of this article. This work was supported by IWT-Vlaanderen, personal fellowship PS, FWO Vlaanderen and KU Leuven grant GOA2008/16. We wish to thank Sandra Meulemans for technical assistance, Fred Van Leuven for advice and Robert Day, Ann White and Iris Lindberg for providing materials.

REFERENCES

1 Jackson RS, Creemers JW, Ohagi S, Raffin-Sanson ML, Sanders L, Montague CT *et al.* Obesity and impaired prohormone processing associated with mutations in the human prohormone convertase 1 gene. *Nat Genet* 1997; **16**: 303–306.
2 Montague CT, Farooqi IS, Whitehead JP, Soos MA, Rau H, Wareham NJ *et al.* Congenital leptin deficiency is associated with severe early-onset obesity in humans. *Nature* 1997; **387**: 903–908.
3 Seidah NG, Sadr MS, Chrétien M, Mbikay M. The multifaceted proprotein convertases: their unique, redundant, complementary, and opposite functions. *J Biol Chem* 2013; **288**: 21473–21481.
4 Creemers JWM, Khatib A-M. Knock-out mouse models of proprotein convertases: unique functions or redundancy? *Front Biosci* 2008; **13**: 4960–4971.
5 Lindberg I. Evidence for cleavage of the PC1/PC3 pro-segment in the endoplasmic reticulum. *Mol Cell Neurosci* 1994; **5**: 263–268.
6 Farooqi IS, Volders K, Stanhope R, Heuschkel R, White A, Lank E *et al.* Hyperphagia and early-onset obesity due to a novel homozygous missense mutation in prohormone convertase 1/3. *J Clin Endocrinol Metab* 2007; **92**: 3369–3373.
7 Strawbridge RJ, Dupuis J, Prokopenko I, Barker A, Ahlqvist E, Rybin D *et al.* Genome-wide association identifies nine common variants associated with fasting proinsulin levels and provides new insights into the pathophysiology of type 2 diabetes. *Diabetes* 2011; **60**: 2624–2634.
8 Corpeleijn E, Petersen L, Holst C, Saris WH, Astrup A, Langin D *et al.* Obesity-related polymorphisms and their associations with the ability to regulate fat oxidation in obese Europeans: the NUGENOB study. *Obesity (Silver Spring)* 2010; **18**: 1369–1377.
9 Goossens GH, Petersen L, Blaak EE, Hul G, Arner P, Astrup *et al.* Several obesity- and nutrient-related gene polymorphisms but not FTO and UCP variants modulate postabsorptive resting energy expenditure and fat-induced thermogenesis in obese individuals: the NUGENOB study. *Int J Obes (Lond)* 2009; **33**: 669–679.
10 Gjesing AP, Vestmar MA, Jørgensen T, Heni M, Holst JJ, Witte DR *et al.* The effect of PCSK1 variants on waist, waist-hip ratio and glucose metabolism is modified by sex and glucose tolerance status. *PLoS One* 2011; **6**: e23907.
11 Stijnen P, Tuand K, Varga TV, Franks PW, Aertgeerts B. Creemers JWM. The association of common variants in PCSK1 with obesity: a HuGE review and meta-analysis. *Am J Epidemiol* 2014; **180**: 1051–1065.
12 Philippe J, Stijnen P, Meyre D, De Graeve F, Thuillier D, Delplanque J *et al.* A nonsense loss-of-function mutation in PCSK1 contributes to dominantly inherited human obesity. *Int J Obes (Lond)* 2014; **39**: 295–302.
13 Creemers JWM, Choquet H, Stijnen P, Vatin V, Pigeyre M, Beckers S *et al.* Heterozygous mutations causing partial prohormone convertase 1 deficiency contribute to human obesity. *Diabetes* 2012; **61**: 383–390.
14 Martín MG, Lindberg I, Solorzano-Vargas RS, Wang J, Avitzur Y, Bandsma R *et al.* Congenital proprotein convertase 1/3 deficiency causes malabsorptive diarrhea and other endocrinopathies in a pediatric cohort. *Gastroenterology* 2013; **145**: 138–148.
15 Jackson RS, Creemers JWM, Farooqi IS, Raffin-Sanson M-L, Varro A, Dockray GJ *et al.* Small-intestinal dysfunction accompanies the complex endocrinopathy of human proprotein convertase 1 deficiency. *J Clin Invest* 2003; **112**: 1550–1560.
16 Bandsma RHJ, Sokollik C, Chami R, Cutz E, Brubaker PL, Hamilton JK *et al.* From diarrhea to obesity in prohormone convertase 1/3 deficiency: age-dependent clinical, pathologic, and enteroendocrine characteristics. *J Clin Gastroenterol* 2013; **47**: 834–843.
17 Pickett LA, Yourshaw M, Albornoz V, Chen Z, Solorzano-Vargas RS, Nelson SF *et al.* Functional consequences of a novel variant of PCSK1. *PLoS One* 2013; **8**: e55065.
18 Frank GR, Fox J, Candela N, Jovanovic Z, Bochukova E, Levine J *et al.* Severe obesity and diabetes insipidus in a patient with PCSK1 deficiency. *Mol Genet Metab* 2013; **110**: 191–194.
19 Wilschanski M, Abbasi M, Blanco E, Lindberg I, Yourshaw M, Zangen D *et al.* A novel familial mutation in the PCSK1 gene that alters the oxyanion hole residue of proprotein convertase 1/3 and impairs its enzymatic activity. *PLoS One* 2014; **9**: e108878.
20 Zhu X, Zhou A, Dey A, Norrbom C, Carroll R, Zhang C *et al.* Disruption of PC1/3 expression in mice causes dwarfism and multiple neuroendocrine peptide processing defects. *Proc Natl Acad Sci USA* 2002; **99**: 10293–10298.
21 Lloyd DJ, Bohan S, Gekakis N. Obesity, hyperphagia and increased metabolic efficiency in Pc1 mutant mice. *Hum Mol Genet* 2006; **15**: 1884–1893.
22 Strausberg SL, Alexander PA, Gallagher DT, Gilliland GL, Barnett BL, Bryan PN. Directed evolution of a subtilisin with calcium-independent stability. *Biotechnology (N Y)* 1995; **13**: 669–673.
23 Lemaire K, Ravier MA, Schraenen A, Creemers JWM¸ Van de Plas R, Granvik M *et al.* Insulin crystallization depends on zinc transporter ZnT8 expression, but is not required for normal glucose homeostasis in mice. *Proc Natl Acad Sci USA* 2009; **106**: 14872–14877.
24 Brouwers B, de Faudeur G, Osipovich AB, Goyvaerts L, Lemaire K, Boesmans L *et al.* Impaired islet function in commonly used transgenic mouse lines due to human growth hormone minigene expression. *Cell Metab* 2014; **20**: 979–990.
25 Blanco EH, Peinado JR, Martín MG, Lindberg I. Biochemical and cell biological properties of the human prohormone convertase 1/3 Ser357Gly mutation: a PC1/3 hypermorph. *Endocrinology* 2014; **155**: 3434–3447.
26 Campeau E, Ruhl VE, Rodier F, Smith CL, Rahmberg BL, Fuss JO *et al.* A versatile viral system for expression and depletion of proteins in mammalian cells. *PLoS One* 2009; **4**: e6529.
27 Scheuner D, Vander Mierde D, Song B, Flamez D, Creemers JWM, Tsukamoto K *et al.* Control of mRNA translation preserves endoplasmic reticulum function in beta cells and maintains glucose homeostasis. *Nat Med* 2005; **11**: 757–764.

28 Subramanian A, Tamayo P, Mootha VK, Mukherjee S, Ebert BL, Gillette MA *et al.* Gene set enrichment analysis: a knowledge-based approach for interpreting genome-wide expression profiles. *Proc Natl Acad Sci USA* 2005; **102**: 15545–15550.
29 Merico D, Isserlin R, Stueker O, Emili A, Bader GD. Enrichment map: a network-based method for gene-set enrichment visualization and interpretation. *PLoS One* 2010; **5**: e13984.
30 Saeed AI, Sharov V, White J, Li J, Liang W, Bhagabati N *et al.* TM4: a free, open-source system for microarray data management and analysis. *Biotechniques* 2003; **34**: 374–378.
31 Janky R, Verfaillie A, Imrichová H, Van de Sande B, Standaert L, Christiaens V *et al.* iRegulon: from a gene list to a gene regulatory network using large motif and track collections. *PLoS Comput Biol* 2014; **10**: e1003731.
32 Andersen CL, Jensen JL, Ørntoft TF. Normalization of real-time quantitative reverse transcription-PCR data: a model-based variance estimation approach to identify genes suited for normalization, applied to bladder and colon cancer data sets. *Cancer Res* 2004; **64**: 5245–5250.
33 Hellemans J, Mortier G, De Paepe A, Speleman F, Vandesompele J. qBase relative quantification framework and software for management and automated analysis of real-time quantitative PCR data. *Genome Biol* 2007; **8**: R19.
34 Benzinou M, Creemers JWM, Choquet H, Lobbens S, Dina C, Durand E *et al.* Common nonsynonymous variants in PCSK1 confer risk of obesity. *Nat Genet* 2008; **40**: 943–945.
35 Kondo S, Saito A, Asada R, Kanemoto S, Imaizumi K. Physiological unfolded protein response regulated by OASIS family members, transmembrane bZIP transcription factors. *IUBMB Life* 2011; **63**: 233–239.
36 Hebert DN, Bernasconi R, Molinari M. ERAD substrates: which way out? *Semin Cell Dev Biol* 2010; **21**: 526–532.
37 Määttänen P, Gehring K, Bergeron JJM, Thomas DY. Protein quality control in the ER: the recognition of misfolded proteins. *Semin Cell Dev Biol* 2010; **21**: 500–511.
38 Zandberg WF, Benjannet S, Hamelin J, Pinto BM, Seidah NG. N-glycosylation controls trafficking, zymogen activation and substrate processing of proprotein convertases PC1/3 and subtilisin kexin isozyme-1. *Glycobiology* 2011; **21**: 1290–1300.
39 Shental-Bechor D, Levy Y. Effect of glycosylation on protein folding: a close look at thermodynamic stabilization. *Proc Natl Acad Sci USA* 2008; **105**: 8256–8261.
40 Prabhu Y, Blanco EH, Liu M, Peinado JR, Wheeler MC, Gekakis N *et al.* Defective transport of the obesity mutant PC1/3 N222D contributes to loss of function. *Endocrinology* 2014; **155**: 2391–2401.
41 Zhou Y, Lindberg I. Enzymatic properties of carboxyl-terminally truncated prohormone convertase 1 (PC1/SPC3) and evidence for autocatalytic conversion. *J Biol Chem* 1994; **269**: 18408–18413.
42 Geva Y, Schuldiner M. The back and forth of cargo exit from the endoplasmic reticulum. *Curr Biol* 2014; **24**: R130–R136.
43 Hoshino A, Kowalska D, Jean F, Lazure C, Lindberg I. Modulation of PC1/3 activity by self-interaction and substrate binding. *Endocrinology* 2011; **152**: 1402–1411.
44 Arias a E, Vélez-Granell CS, Mayer G, Bendayan M. Colocalization of chaperone Cpn60, proinsulin and convertase PC1 within immature secretory granules of insulin-secreting cells suggests a role for Cpn60 in insulin processing. *J Cell Sci* 2000; **113**: 2075–2083.
45 Creemers JW, van de Loo JW, Plets E, Hendershot LM, Van De Ven WJ. Binding of BiP to the processing enzyme lymphoma proprotein convertase prevents aggregation, but slows down maturation. *J Biol Chem* 2000; **275**: 38842–38847.
46 Gyamera-Acheampong C, Sirois F, Denis NJ, Mishra P, Figeys D, Basak *et al.* The precursor to the germ cell-specific PCSK4 proteinase is inefficiently activated in transfected somatic cells: evidence of interaction with the BiP chaperone. *Mol Cell Biochem* 2011; **348**: 43–52.
47 Cakir I, Cyr NE, Perello M, Litvinov BP, Romero A, Stuart RC *et al.* Obesity induces hypothalamic endoplasmic reticulum stress and impairs proopiomelanocortin (POMC) post-translational processing. *J Biol Chem* 2013; **288**: 17675–17688.
48 Zhu J, Bultynck G, Luyten T, Parys JB, Creemers JWM, Van de Ven WJM *et al.* Curcumin affects proprotein convertase activity: Elucidation of the molecular and subcellular mechanism. *Biochim Biophys Acta* 2013; **1833**: 1924–1935.
49 Liew CW, Assmann A, Templin AT, Raum JC, Lipson KL, Rajan S *et al.* Insulin regulates carboxypeptidase E by modulating translation initiation scaffolding protein eIF4G1 in pancreatic β cells. *Proc Natl Acad Sci USA* 2014; **111**: E2319–E2328.
50 Shen FS, Loh YP. Intracellular misrouting and abnormal secretion of adrenocorticotropin and growth hormone in cpefat mice associated with a carboxypeptidase E mutation. *Proc Natl Acad Sci USA* 1997; **94**: 5314–5319.

Supplementary Information accompanies this paper on International Journal of Obesity website (http://www.nature.com/ijo)